A J INTEGRAL ANALYSIS FOR THE COMPACT SPECIMEN, CONSIDERING AXIAL FORCE AS WELL AS BENDING EFFECTS*

J. G. Merkle

Oak Ridge National Laboratory
Oak Ridge, Tennessee 37830

H. T. Corten

Department of Theoretical and Applied Mechanics
University of Illinois
Urbana, Illinois 61801

Abstract

An important fracture mechanics problem is the determination of fracture toughness values with small specimens that fail after yielding. The J Integral has an explicit meaning in terms of notch tip conditions in the plastic range and can be calculated from single specimen test data. In this paper, an improved J Integral analysis is developed for the Compact specimen by considering the combined loading that exists on the net section. The analysis agrees with linear elastic fracture mechanics in the elastic range and gives a result close to that given by the Equivalent Energy Method in the plastic range.

*Research sponsored by the U.S. Atomic Energy Commission under contract with Union Carbide Corporation.

Nomenclature

A_c	Crack area, in.^{2}
a	Crack length, in.
B	Specimen thickness, in.
b	Ligament width, in.
c	Half the ligament width, in.
E	Modulus of elasticity, ksi.
G_I	Elastic strain energy release rate for plane strain conditions, in.-kips/in.^{2}
g	Function of the plastic angle of rotation due to the crack, dimensionless
J	The J Integral, in.-kips/in.^{2}
J_c	Critical value of the J Integral, in.-kips/in.^{2}
J_o	Value of the J Integral for a point on the linear portion of the load-displacement curve, in.-kips/in.^{2}
J_p	Plastic portion of the J Integral, in.-kips/in.^{2}
K_c	Critical value of the elastic crack tip stress intensity factor, ksi $\cdot$ in.$^{1/2}$
K_o	Value of the elastic crack tip stress intensity factor for a point on the linear portion of the load-displacement curve, ksi $\cdot$ in.$^{1/2}$
K_I	The elastic crack tip stress intensity factor for plane strain conditions, ksi $\cdot$ in.$^{1/2}$
K_{Icd}	Fracture toughness computed according to the Equivalent Energy Method, ksi $\cdot$ in.$^{1/2}$
k	Elastic stiffness, kips/in.
M_{fp}	Fully plastic bending moment, in.-kips
m	Function defined by Eq. (57), dimensionless

P	Force, kips
P_{fp}	Fully plastic load, kips
P_o	Load at a point on the linear portion of the load-displacement curve, kips
P_Y	Load at the proportional limit of the load-displacement curve, kips
W	Width of a Compact specimen, in.
Y	Shape factor for the Compact specimen; also sometimes denoted by $f(a/W)$; dimensionless
α	Ratio of the width of the internal stress block equilibrating the applied load at plastic collapse, to the ligament width, dimensionless
β	Stiffness coefficient, dimensionless
Δ	Total displacement of the applied load due to the crack, in.
Δ_E	Elastic displacement of the applied load due to the crack, in.
Δ_o	Total displacement of the applied load due to the crack, for a point on the linear portion of the load-displacement curve, in.
Δ_P	Plastic displacement of the applied load due to the crack, in.
Δ_Y	Total displacement of the applied load due to the crack, at the proportional limit of the load-displacement curve, in.
δ	Crack tip opening displacement, in.
δ_E	Elastic portion of the crack tip opening displacement, in.
δ_P	Plastic portion of the crack tip opening displacement, in.
η_c	Complementary energy coefficient, dimensionless
η_r	Real energy coefficient, dimensionless
θ	Angle of rotation due to the crack, radians
θ_E	Elastic angle of rotation due to the crack, radians
θ_P	Plastic angle of rotation due to the crack, radians
λ_E	Coefficient for computing G_I, for elastic conditions; also used for computing K_{Icd}^2/E for elastic-plastic conditions; dimensionless

λ_J Coefficient for computing J, for elastic conditions, dimensionless

σ_Y Yield stress, ksi

ϕ_c Complementary energy per unit thickness, kips

ϕ_o Real energy per unit thickness, for a point on the linear portion of the load-displacement curve, kips

ϕ_r Real energy per unit thickness, kips

Introduction

One of the most important existing problems in the field of applied fracture mechanics is the calculation of correct values of fracture toughness from small specimen test records. In many cases, specimens large enough to provide "valid" fracture toughness values cannot be obtained from the product form of interest. In other cases, large enough specimens can be obtained, but preparing and testing them is impractical because of limitations related to size and/or cost. Unlike large specimens that give "valid" fracture toughness values, small specimens usually fail after rather than before the onset of gross yielding. Therefore, a method for obtaining correct values of fracture toughness from non-linear load-displacement records is needed in order to make the application of fracture mechanics more practical.

The requirements of a satisfactory method for calculating fracture toughness values from non-linear load-displacement records include the following:

1. The quantity representing fracture toughness should be expressed completely in terms of measurable quantities.

2. The calculated quantity should have an explicit meaning in terms of notch tip conditions.

3. The method of calculation should be analytically derived from the principles of solid mechanics, for nonlinear conditions, using a minimum number of simplifying assumptions.

4. The calculation should agree with linear elastic fracture mechanics, for the case of a specimen failing in the linear range of its load-displacement curve.

Several approaches to the problem of calculating fracture toughness values from inelastic load-displacement records obtained from small specimens have been proposed. These methods can be classified as follows:

1. Correlations;
2. Semi-empirical methods
   (a) Energy and displacement relationships,
   (b) Relationships between material properties and fracture toughness;
3. Analytical methods.

At present, correlations are proving extremely useful, but their applicability to new materials and to changed material conditions is uncertain. Energy and displacement relationships are apt to lack a general analytical basis, and some have no definite meaning in terms of notch tip conditions. Relationships between material properties and fracture toughness are intriguing, but they turn out to be dependent upon small microstructural dimensions that are difficult or impossible to measure directly. Analytical methods offer the most promise of success in the long run, because they stand the best chance of meeting all of the requirements of a satisfactory method stated above.

The J Integral, derived by Rice,[1,2] is presently the only analytically based inelastic fracture criterion under development. The J Integral is the rate of change of total potential energy with respect to crack surface area. It is an analytical generalization, for nonlinear conditions, of the elastic strain energy release rate, G_I. It also represents the integral of the total strain energy density around the crack tip contour.[1]

Initial experiments by Begley and Landes,[3,4] using several series of geometrically identical specimens with incrementally different crack lengths,

have demonstrated the feasibility of using the J Integral as a fracture criterion. Recently, analyses have been developed for calculating the value of the J Integral from a single load-displacement curve.[5,6] At present, the Compact* specimen is being treated as a deeply cracked beam in pure bending, using the equation[6]

$$J = \frac{2}{b} \int_0^{\Delta} \left(\frac{P}{B}\right) d\Delta \quad , \tag{1}$$

where b is the length of the uncracked ligament ahead of the crack tip, B is the specimen thickness, P is the total load on the specimen, and Δ is the displacement of the load due to the crack. However, it appears that Eq. (1) is somewhat conservative with respect to linear elastic fracture mechanics, for the Compact specimen, for failure in the linear range of the load-displacement curve. The purpose of the analysis to be presented here is to investigate the effect of the axial force, acting in combination with the bending moment, on the value of the J Integral for the Compact specimen. The results indicate that considering the effects of the axial force leads to much better agreement between the value of the J Integral and the value of G_I, for linear elastic conditions.

The analysis to be presented here consists of the derivation of the fully plastic limit load conditions for a Compact specimen, followed by the derivation of an expression for the J Integral, for the same specimen, based on the assumption that the plastic displacement of the load due to the crack is a function of the ratio of the applied load to the fully plastic limit load. Numerical comparisons are then made between the value of the J Integral and the value of G_I, for linear elastic conditions. The results

*Formerly known as the Compact Tension specimen.

indicate that, for the Compact specimen, the formula derived here is a significant improvement over the formula for J based on the assumption that the uncracked ligament is loaded in pure bending.

Plastic Limit Analysis of a Compact Specimen

The fully plastic limit load conditions in a Compact specimen can be analyzed with the aid of the familiar interaction equation that relates the axial force and the bending moment at plastic collapse for a member of rectangular cross section.[7] However, for this study, an alternate analysis was developed and used because it provides the value of a single geometric coefficient that solely determines the effect of the axial force on the value of the J Integral for the Compact specimen. Referring to Fig. 1, it can be seen that the internal resisting moment at plastic collapse in a Compact specimen is given by

$$M_{fp} = \sigma_Y B c^2 (1 - \alpha^2) \quad , \tag{2}$$

and that the applied load at plastic collapse is given by

$$P_{fp} = \sigma_Y B c (2\alpha) \quad , \tag{3}$$

where σ_Y is the yield stress, B is the specimen thickness, c is half the distance from the crack tip to the back face, and α is the dimensionless coefficient that determines the width of the internal stress block required to equilibrate the applied load P_{fp}. The fully plastic moment is also the moment of the applied load P_{fp} about the centroid of the net section, so that

$$M_{fp} = P_{fp} (a + c) \quad . \tag{4}$$

Equating the expressions for M_{fp} given by Eqs. (2) and (4), and using Eq. (3) gives

$$\alpha^2 + 2\left(\frac{a}{c} + 1\right)\alpha - 1 = 0 \quad . \tag{5}$$

Solving Eq. (5) for α gives

$$\alpha = \left[\left(\frac{a}{c}\right)^2 + 2\left(\frac{a}{c}\right) + 2\right]^{1/2} - \left(\frac{a}{c} + 1\right) \quad . \tag{6}$$

It will be shown subsequently that α is the coefficient that determines the effect of the axial force on the value of the J Integral for the Compact specimen. It should be noted that Eqs. (2) through (5) are based on a lower bound plastic limit analysis of the net section, ignoring the stress triaxiality caused by the crack tip. The justification for this approach, based on a comparison between the lower bound limit analysis and an upper bound limit analysis that considers the stress triaxiality caused by the crack tip, is given in Appendix A.

The displacement diagram at plastic collapse for a Compact specimen is shown in Fig. 2. Noting that rotations occur about the point of stress reversal, the plastic angle of rotation θ_p is defined, in terms of the plastic load point displacement, by

$$\theta_p = \frac{\Delta_p}{a + (1 + \alpha)\, c} \quad , \tag{7}$$

and in terms of the plastic crack tip opening displacement by

$$\theta_p = \frac{\delta_p}{(1 + \alpha)\, c} \quad . \tag{8}$$

In Eqs. (7) and (8), Δ_p and δ_p are the plastic load point and crack tip opening displacements, respectively. Equating the expressions for θ_p given by Eqs. (7) and (8), and using the substitution

$$a = W - 2c \quad , \tag{9}$$

where W is the specimen width as defined in Fig. 2, gives

$$\Delta_P = \frac{\left(\frac{W}{c} + \alpha - 1\right)}{(1 + \alpha)} \delta_P \quad . \tag{10}$$

J Integral Analysis

The starting point for this analysis is the same as the one used in Ref. 6, namely the definition of the J Integral as the area, per unit increase in crack surface area, between two load-displacement curves for two geometrically identical specimens with incrementally different crack sizes. Referring to Fig. 3, this area can be represented as the sum of the areas of a series of differential parallelograms, one of which is shown shaded in Fig. 3. The area of one of these differential parallelograms is related to the value of the J Integral by the expression

$$(dJ)(dA_c) = - \left(\frac{\partial \Delta}{\partial A_c}\right)_P dA_c \left(\frac{\partial P}{\partial A_c}\right)_{\Delta_P} dA_c \quad , \tag{11}$$

where J is the value of the J Integral, A_c is the crack surface area, P is the applied load, Δ and Δ_P are the total and the plastic displacements of the applied load due to the crack, respectively, and the subscripts P and Δ_P following the partial derivatives indicate the variable that is held constant during partial differentiation. The total and the plastic displacements are related by the equation

$$\Delta = \Delta_E + \Delta_P \quad , \tag{12}$$

where Δ_E is the elastic displacement of the applied load due to the crack. Substituting Eq. (12) into Eq. (11), separating the elastic and the plastic terms, dividing both sides by dA_c and

choosing the subsequently most convenient variable of integration for each term gives

$$dJ = \left(\frac{\partial \Delta_E}{\partial A_c}\right)_P \cdot dP - \left(\frac{\partial P}{\partial A_c}\right)_{\Delta_P} \cdot d\Delta_P \quad . \tag{13}$$

The elastic displacement Δ_E can be written as

$$\Delta_E = \frac{P}{k} \quad , \tag{14}$$

where k is the elastic stiffness, which is independent of P. Therefore, substituting Eq. (14) into Eq. (13), using the relationship

$$A_c = Ba \quad , \tag{15}$$

and integrating both sides of the resulting equation gives

$$J = \frac{1}{2}\frac{P^2}{B}\frac{\partial\left(\frac{1}{k}\right)}{\partial a} - \frac{1}{B}\int_o^{\Delta_P}\left(\frac{\partial P}{\partial a}\right)_{\Delta_P} d\Delta_P \quad . \tag{16}$$

The first term in Eq. (16) can be recognized as the elastic strain energy release rate, G_I. The second term, the value of which reduces to zero for linear elastic behavior, is the increase in J over G_I caused by nonlinear behavior, and it will be denoted here by the symbol J_P. Thus,

$$J_P = -\frac{1}{B}\int_o^{\Delta_P}\left(\frac{\partial P}{\partial a}\right)_{\Delta_P} d\Delta_P \quad . \tag{17}$$

The value of J_P will be positive because the value of $(\partial P/\partial a)_{\Delta_P}$ is negative.

Following the approach taken by Rice,[6] the integral in Eq. (17) will be evaluated by assuming that the plastic angle of rotation θ_p is a function only of the ratio of the applied load P to the fully plastic collapse load P_{fp}. For application to Eq. (17), this function will be written in its inverse form, namely

$$P = P_{fp}\, g\,(\theta_p) \quad . \tag{18}$$

Using Eq. (9), the partial derivative in Eq. (17) can be written as

$$-\left(\frac{\partial P}{\partial a}\right)_{\Delta_p} = \frac{1}{2}\left(\frac{\partial P}{\partial c}\right)_{\Delta_p} \quad . \tag{19}$$

Substituting Eq. (18) into Eq. (19) then gives

$$-\left(\frac{\partial P}{\partial a}\right)_{\Delta_p} = \frac{1}{2}\frac{P}{P_{fp}}\left(\frac{\partial P_{fp}}{\partial c}\right)_{\Delta_p} + \frac{1}{2} P_{fp}\left(\frac{\partial g}{\partial \theta_p}\right)\left(\frac{\partial \theta_p}{\partial c}\right)_{\Delta_p} \quad . \tag{20}$$

However,

$$\left(\frac{\partial P}{\partial \Delta_p}\right)_c = P_{fp}\left(\frac{\partial g}{\partial \theta_p}\right)\left(\frac{\partial \theta_p}{\partial \Delta_p}\right)_c \quad , \tag{21}$$

so that

$$\left(\frac{\partial g}{\partial \theta_p}\right) = \frac{\left(\frac{\partial P}{\partial \Delta_p}\right)_c}{P_{fp}\left(\frac{\partial \theta_p}{\partial \Delta_p}\right)_c} \quad . \tag{22}$$

Therefore, substituting Eq. (22) into Eq. (20) gives

$$-\left(\frac{\partial P}{\partial a}\right)_{\Delta_P} = \frac{1}{2}\frac{\left(\frac{\partial P_{fp}}{\partial c}\right)_{\Delta_P}}{P_{fp}} P + \frac{1}{2}\frac{\left(\frac{\partial \theta_P}{\partial c}\right)_{\Delta_P}}{\left(\frac{\partial \theta_P}{\partial \Delta_P}\right)_c}\left(\frac{\partial P}{\partial \Delta_P}\right)_c \quad . \tag{23}$$

The evaluation of the first term in Eq. (23) begins with the partial differentiation of Eq. (3) with respect to c, which gives

$$\left(\frac{\partial P_{fp}}{\partial c}\right)_{\Delta_P} = 2\sigma_Y B\left[\alpha + c\frac{\partial \alpha}{\partial c}\right] \quad . \tag{24}$$

Substituting Eq. (9) into Eq. (5) gives

$$\alpha^2 + 2\left[\frac{W}{c} - 1\right]\alpha - 1 = 0 \quad . \tag{25}$$

Differentiating Eq. (25) and then eliminating (W/c) by substitution from Eq. (25) gives

$$\frac{\partial \alpha}{\partial c} = \frac{1}{c}\frac{(1 + 2\alpha - \alpha^2)\,\alpha}{(1 + \alpha^2)} \quad . \tag{26}$$

By substituting Eq. (26) into Eq. (24) and using

$$b = 2c \tag{27}$$

it follows that

$$\frac{1}{2}\frac{\left(\frac{\partial P_{fp}}{\partial c}\right)_{\Delta_P}}{P_{fp}} = \frac{2}{b}\frac{(1 + \alpha)}{(1 + \alpha^2)} \quad . \tag{28}$$

The evaluation of the second term in Eq. (23) begins with the partial differentiation of Eq. (7) with respect to c which, with the aid of Eq. (26),

gives

$$\left(\frac{\partial \theta_P}{\partial c}\right)_{\Delta_P} = \frac{\Delta_P}{\left[a + (1 + \alpha)\ c\right]^2} \frac{(1 - 2\alpha - \alpha^2)}{(1 + \alpha^2)} \quad . \tag{29}$$

Taking the partial derivative of Eq. (7) with respect to Δ_P gives

$$\left(\frac{\partial \theta_P}{\partial \Delta_P}\right)_c = \frac{1}{\left[a + (1 + \alpha)\ c\right]} \quad . \tag{30}$$

From Eqs. (5) and (27), it follows that

$$\left[a + (1 + \alpha)\ c\right] = \frac{b}{2}\left(\frac{1 + \alpha^2}{2\alpha}\right) \quad . \tag{31}$$

Then, combining Eqs. (29), (30), and (31) gives

$$\frac{1}{2} \frac{\left(\frac{\partial \theta_P}{\partial c}\right) \Delta_P}{\left(\frac{\partial \theta_P}{\partial \Delta_P}\right)_c} = \frac{2}{b}\, \alpha\, \frac{(1 - 2\alpha - \alpha^2)\Delta_P}{(1 + \alpha^2)^2} \quad . \tag{32}$$

Finally, substituting Eqs. (28) and (32) into Eq. (23), and the result into Eq. (17), gives

$$J_P = \frac{2}{b} \frac{(1 + \alpha)}{(1 + \alpha^2)} \int_o^{\Delta_P} \left(\frac{P}{B}\right) d\Delta_P + \frac{2}{b}\, \alpha\, \frac{(1 - 2\alpha - \alpha^2)}{(1 + \alpha^2)^2} \int_o^{\frac{P}{B}} \Delta_P \left(\frac{P}{B}\right) d\left(\frac{P}{B}\right) \quad . \tag{33}$$

Eq. (33) enables the value of the J Integral to be computed from a single Compact specimen load-displacement curve, considering the effect of the axial force acting on the net section, which is neglected by Eq. (1).

For the case of pure bending, $\alpha = o$, and by replacing Δ_P by Δ as discussed in Ref. 6, Eq. (33) reduces to Eq. (1), as it should. The first and

second integrals in Eq. (33) are the real work and the complementary work of the applied load, per unit thickness, respectively. For the rigid plastic case, the complementary work is zero, and the elastic displacements are also zero, so that Eq. (33) becomes

$$J = \frac{2}{b}\frac{(1+\alpha)}{(1+\alpha^2)}\frac{P_{fp}}{B}\Delta \quad . \tag{34}$$

From Eq. (25)

$$\frac{W}{c} + \alpha - 1 = \frac{1+\alpha^2}{2\alpha} \quad , \tag{35}$$

and by substituting Eq. (35) into Eq. (10),

$$\Delta = \frac{(1+\alpha^2)}{2\alpha(1+\alpha)}\delta \quad . \tag{36}$$

Substituting Eqs. (36), (27) and (3) into Eq. (34) then gives

$$J = \sigma_Y \delta \quad , \tag{37}$$

which is the correct expression for the rigid plastic case, for all geometries.

Comparison of Elastic and J Integral Analyses Based on Total Displacement

At the present time, J Integral calculations are being made for the Compact specimen by means of Eq. (1), based on the total displacement of the applied load.[6] As discussed by Rice,[6] this procedure is correct if either the elastic displacement of the applied load due to the crack is negligibly small, or if it also is only a function of the ratio P/P_{fp}. The acceptability of a J Integral calculation based on the total displacement

of the applied load can be evaluated by comparing the J Integral calculation with the known solution for G_I, for linear elastic conditions. This is most easily done by writing both the elastic solution for G_I and the J Integral solution for elastic conditions in the same form as Eq. (1). The elastic solution for a Compact specimen gives

$$K_I = \frac{PY}{B\sqrt{W}} \quad , \tag{38}$$

where Y is the elastically calculated nondimensional shape factor, sometimes denoted[8] by the symbol f(a/W). Squaring both sides of Eq. (38) and dividing by E, the elastic modulus gives

$$\frac{K_I^2}{E} = G_I = \frac{P^2Y^2}{EB^2W} \quad . \tag{39}$$

Using Eqs. (9) and (27), it is convenient to write

$$W = \frac{b}{1 - \frac{a}{W}} \quad , \tag{40}$$

which, when substituted into Eq. (39) gives

$$G_I = \frac{P^2Y^2(1 - \frac{a}{W})}{EB^2b} \quad . \tag{41}$$

For the linear elastic case,

$$\int_o^{\Delta} \left(\frac{P}{B}\right) d\Delta = \frac{P^2}{2Bk} \quad , \tag{42}$$

so that rearranging Eq. (42) gives

$$P^2 = 2Bk \int_o^{\Delta} \left|\frac{P}{B}\right| d\Delta \quad . \tag{43}$$

Substituting Eq. (43) into Eq. (41) gives

$$G_I = \frac{\lambda_E}{b} \int_o^{\Delta} \left|\frac{P}{B}\right| d\Delta \quad , \tag{44}$$

where

$$\lambda_E = 2 \left|\frac{Y^2}{\beta}\right| \left|1 - \frac{a}{w}\right| \quad , \tag{45}$$

and

$$\beta = \frac{EB}{k} \quad . \tag{46}$$

Values of β and Y for the Compact specimen have been calculated by Roberts.[9] Entering these values into Eq. (45) produces the values of λ_E shown in Table 1. It should be noted that the values of λ_E shown in Table 1 all exceed 2.0. For this reason, Eq. (1) is conservative when applied to the Compact specimen in the linear elastic range.

Expressing Eq. (33) for the J Integral in terms of the total displacement of the applied load due to the crack, and using the following substitutions,

$$\eta_r = \frac{2(1 + \alpha)}{(1 + \alpha^2)} \quad , \tag{47}$$

$$\eta_c = \frac{2\alpha(1 - 2\alpha - \alpha^2)}{(1 + \alpha^2)^2} \quad , \tag{48}$$

$$\phi_r = \int_o^{\Delta} \left|\frac{P}{B}\right| d\Delta \quad , \tag{49}$$

$$\phi_c = \int_0^{\frac{P}{B}} \Delta d \left(\frac{P}{B}\right) \quad , \tag{50}$$

gives

$$J = \frac{\left[\eta_r + \eta_c \left(\frac{\phi_c}{\phi_r}\right)\right]}{b} \phi_r \quad . \tag{51}$$

For the linear elastic case, $(\phi_c/\phi_r) = 1$, and Eq. (51) can be written as

$$J = \frac{\lambda_J}{b} \int_0^{\Delta} \left(\frac{P}{B}\right) d\Delta \quad , \tag{52}$$

where

$$\lambda_J = \eta_r + \eta_c \quad . \tag{53}$$

Values of λ_J, and the ratio λ_E / λ_J, are listed in Table 2. The ratio λ_E / λ_J is essentially unity for $a/W \geq 0.5$, indicating that J may be computed from Eq. (33), based on the total displacement of the applied load due to the crack, for $a/W \geq 0.5$. For $a/W < 0.5$, the elastic and the plastic displacements should be considered separately, using Eq. (16).

Calculations of K_c from J Integral Test Data

The expression of fracture toughness in the units of the elastic crack tip stress intensity factor, ksi·in.$^{\frac{1}{2}}$, is well established and useful. This is easily done with the foregoing equations, and in the process, inaccuracies caused by errors in the load point displacement calibration factor can be eliminated. Referring to Fig. 4, the value of J_o for an arbitrarily chosen

point on the linear portion of the load-displacement curve can be written as

$$J_o = \frac{\lambda_J}{b} \phi_o \quad , \tag{54}$$

where

$$\phi_o = \frac{P_o \Delta_o}{2B} \quad . \tag{55}$$

For conditions at the onset of fracture, dividing Eq. (51) by Eq. (54) gives

$$\frac{J_c}{J_o} = m \left(\frac{\phi_r}{\phi_o} \right) \quad , \tag{56}$$

where

$$m = \frac{\eta_r + \eta_c \left(\frac{\phi_c}{\phi_r} \right)}{\lambda_J} \quad , \tag{57}$$

and

$$\frac{\phi_c}{\phi_r} = \frac{P\Delta}{\int_o^\Delta P d\Delta} - 1 \quad . \tag{58}$$

Since

$$\frac{J_c}{J_o} = \left(\frac{K_c}{K_o} \right)^2 \quad , \tag{59}$$

it follows that

$$\frac{K_c}{K_o} = \sqrt{m \left(\frac{\phi_r}{\phi_o} \right)} \quad , \tag{60}$$

where

$$\frac{\phi_r}{\phi_o} = \frac{\int_o^{\Delta} P d\Delta}{\frac{P_o \Delta_o}{2}} \quad . \tag{61}$$

Since the point P_o lies on the linear portion of the load-displacement curve, it also follows that

$$K_o = \frac{P_o Y}{B\sqrt{W}} \quad . \tag{62}$$

Therefore, combining Eqs. (60) and (62) gives

$$K_c = \frac{P_o Y}{B\sqrt{W}} \sqrt{m\left(\frac{\phi_r}{\phi_o}\right)} \quad . \tag{63}$$

Note that Eq. (63) is independent of the displacement calibration factor. The only difference between Eq. (63) and the Equivalent Energy equation for calculating K_{Icd} values developed by Witt and Mager[10, 11] is in the value of m. For a J Integral calculation, m is a variable having a value equal to or less than unity. For an Equivalent Energy calculation, it is arbitrarily assumed that m = 1. It follows that there is no difference between the two calculations for the case of pure bending, because for this case, $\eta_c = 0$ and m = 1.

For points lying between the proportional limit and the maximum load point of a typical experimentally measured[10] Compact specimen load-displacement curve shown in Fig. 5, values of the ratio $(K_{Icd}^2/E) \div J$ are listed in Table 3. The ratio is 1.00 at the proportional limit, and increases to a

value of 1.08 at the maximum load point. Thus, fracture toughness values calculated from Compact specimen data by the J Integral method and by the Equivalent Energy method will always be in close agreement, provided that the same measurement point is used for both calculations. The J Integral method will always give a slightly lower value than the Equivalent Energy method in the nonlinear range, and the two methods will agree exactly in the linear range. Thus, the foregoing analysis resolves, for practical purposes, the differences that have heretofore appeared to exist between the elastic, J Integral, and Equivalent Energy analyses of the Compact specimen.

References

1. J. R. Rice, "Mathematical Analysis in the Mechanics of Fracture," Chapter 3 in Volume 2 of Fracture, an Advanced Treatise, H. Liebowitz, editor, Academic Press, 1968.

2. J. R. Rice, "A Path Independent Integral and the Approximate Analysis of Strain Concentration by Notches and Cracks," Journal of Applied Mechanics, ASME, June 1968, pp. 379 - 386.

3. J. A. Begley and J. D. Landes, "The J Integral as a Fracture Criterion," in Fracture Toughness, Proceedings of the 1971 National Symposium on Fracture Mechanics, Part II, ASTM STP 514, ASTM, 1972, pp. 1 - 23.

4. J. D. Landes and J. A. Begley, "The Effect of Specimen Geometry on J_{Ic}," in Fracture Toughness, Proceedings of the 1971 National Symposium on Fracture Mechanics, Part II, ASTM STP 514, ASTM, 1972, pp. 24-39.

5. R. J. Bucci, P. C. Paris, J. D. Landes and J. R. Rice, "J Integral Estimation Procedures," in Fracture Toughness, Proceedings of the 1971 National Symposium on Fracture Mechanics, Part II, ASTM STP 514, ASTM, 1972, pp. 40 - 69.

6. J. R. Rice, P. C. Paris and J. G. Merkle, "Further Results on J Integral Analysis and Estimates" in Progress in Flaw Growth and Fracture Toughness Testing, Proceedings of the 1972 National Symposium on Fracture Mechanics, ASTM STP 536, ASTM, 1973, pp.

7. G. Winter, "Fundamentals of Member Performance," Chapter 4 in Steel Structures, by W. McGuire, Prentice-Hall, 1968.

8. "Tentative Method of Test for Plane-Strain Fracture Toughness of Metallic Materials," ASTM E 399-70T.

9. E. Roberts, Jr., "Elastic Crack-Edge Displacements for the Compact Tension Specimen," Materials Research and Standards, ASTM, Vol. 9 (2), February 1969, p. 27.

10. F. J. Witt and T. R. Mager, "Fracture Toughness K_{Icd} Values at Temperatures up to 550°F for ASTM A 533 Grade B, Class 1 Steel," Nuclear Engineering and Design, Vol. 17 (1), pp. 91 - 102, August 1971.

11. F. J. Witt and T. R. Mager, "A Procedure for Determining Bounding Values on Fracture Toughness K_{Ic} at Any Temperature," ORNL-TM-3894, Oak Ridge National Laboratory, Oak Ridge, Tennessee, October 1972.

12. C. R. Calladine, "Engineering Plasticity," Pergamon Press, 1969.

13. J. R. Rice, "The Line Spring Model for Surface Flaws," pp. 171-185 in The Surface Crack: Physical Problems and Computational Solutions, ASME, New York, 1972.

14. A. P. Green and B. B. Hundy, "Initial Plastic Yielding in Notch Bend Bars," J. Mech. Phys. Solids, Vol. 4, pp. 128-144, 1956.

Appendix A: Comments Concerning Plastic Limit Analyses for the Compact Specimen

In this paper the plastic limit load and the limit moment for a Compact specimen, as given by Eqs. (2) and (3), are estimated by the Lower Bound Theorem of limit analysis, based on equilibrium.[12] The resulting equations are algebraically simple and easy to apply to a J Integral analysis. However, the accuracy of these Lower Bound equations needs to be evaluated, in order to insure that they do not cause systematic errors in the J Integral analysis. This question can be investigated by means of a comparison between the Lower Bound solution and Rice's Upper Bound solution for an edge cracked specimen,[13] based on an assumed plastic collapse mechanism.[12] This solution is easily adapted to the Compact specimen by defining the line of action of the load as the cracked edge of the specimen. Rice[13] determined the Upper Bound interaction diagram between the normalized axial force and the normalized bending moment at plastic collapse by drawing the interior envelope to a series of tangents, each located by calculation. His graphical solution does not appear to agree exactly with the Green and Hundy[14] solution for pure bending, but a modification to the interior envelope based on the normality rule of plasticity produces the desired agreement. Rice[13] also fit an ellipse within the graphically determined Upper Bound envelope, because the equation of the envelope itself was not determined.

Bucci et al[5] compared some Compact specimen limit load values measured experimentally by Westinghouse with values predicted by Rice's graphically determined interaction diagram. The predicted values were slightly higher than the measured values, as should be the case for an Upper Bound analysis. As shown in Fig. A.1, we found that the same experimental data are bounded

equally well from below by an adjusted Lower Bound curve which is obtained by multiplying the Lower Bound limit load values by the plastic constraint factor of 1.26, which was obtained by Green and Hundy[14] for a notched beam loaded in pure bending. Note that Fig. A.1 is Fig. 10 from Ref. 5, with the adjusted Lower Bound curve added. Since multiplying the yield stress by a constant factor has no effect on the J Integral solution given by Eq. (33), the use of a Lower Bound limit load solution in this analysis appears to be well justified. Note that the rigid-plastic value of J, given by Eq. (37), is numerically affected by the plastic constraint factor. In addition, not shown in Fig. A.1 is the curve corresponding to Rice's elliptical approximation,[13] which passes through the higher data points and falls below the adjusted Lower Bound curve for $0.7 < a/W < 1.0$.

Table 1. Values of Y, β, and λ_E for the Compact Specimen

$\frac{a}{W}$	Y	β	λ_E
0.30	5.85	14.48	3.32
0.35	6.54	18.41	3.12
0.40	7.33	23.22	2.78
0.45	8.34	29.27	2.60
0.50	9.60	37.2	2.48
0.55	11.26	47.9	2.38
0.60	13.62	63.2	2.36
0.65	16.84	85.8	2.32
0.70	21.56	119.8	2.32

Note: Values of Y and β are from Ref. 9.

Table 2. J Integral Analysis Parameters for the Compact Specimen

$\frac{a}{W}$	α	η_r	η_c	λ_J	λ_E	λ_E/λ_J
0.30	0.25	2.352	0.194	2.55	3.32	1.3
0.35	0.23	2.336	0.202	2.54	3.12	1.2
0.40	0.21	2.318	0.206	2.52	2.78	1.1
0.45	0.18	2.284	0.206	2.49	2.60	1.0
0.50	0.16	2.262	0.198	2.46	2.48	1.0
0.55	0.14	2.238	0.188	2.43	2.38	1.0
0.60	0.12	2.206	0.174	2.38	2.36	1.0
0.65	0.10	2.178	0.156	2.33	2.32	1.0
0.70	0.09	2.164	0.144	2.31	2.32	1.0

Table 3. Values of $(K_{Icd}^2 / E) \div J$ for Measurement Points in the Plastic Range of the Load-Displacement Curve for a Compact Specimen of A533 Grade B Class 1 Steel, a/W = 0.5.

$\frac{\Delta}{\Delta_Y}$	$\frac{P}{P_Y}$	$\frac{\phi_c}{\phi_r}$	$\frac{(K_{Icd}^2 / E)}{J}$
1.00	1.00	1.000	1.00
1.50	1.22	0.749	1.02
2.00	1.38	0.619	1.03
2.50	1.50	0.547	1.04
3.00	1.55	0.459	1.05
3.50	1.59	0.402	1.05
4.00	1.63	0.365	1.06
5.00	1.68	0.306	1.06
6.00	1.70	0.255	1.07
7.00	1.72	0.225	1.07
8.00	1.73	0.196	1.07
9.00	1.74	0.179	1.07
10.00	1.75	0.163	1.08

Figure Captions

Fig. 1. Stress conditions in a Compact specimen at plastic collapse.

Fig. 2. Displacement diagram for a Compact specimen at plastic collapse.

Fig. 3. Definition of the incremental area between two load-displacement curves that is related to the J Integral.

Fig. 4. Schematic load per unit thickness versus displacement diagram, showing the definitions of P_o, Δ_o and ϕ_o.

Fig. 5. Typical normalized load-displacement diagram for a Compact specimen.

Fig. A.1. Upper bound and adjusted lower bound limit loads divided by BW as a function of dimensionless crack size, a/W, for Westinghouse A533B Compact specimen.

ORNL – DWG 74 – 107

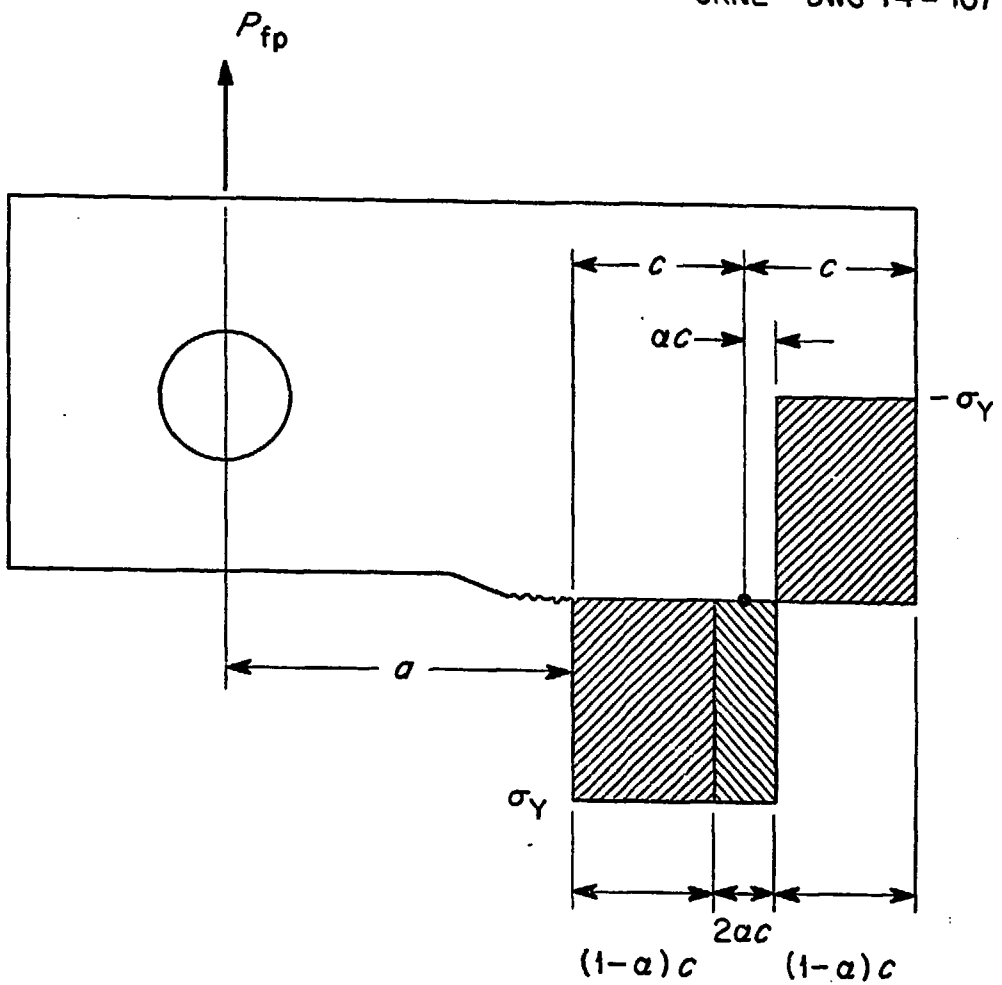

Figure 1

ORNL-DWG 74-111

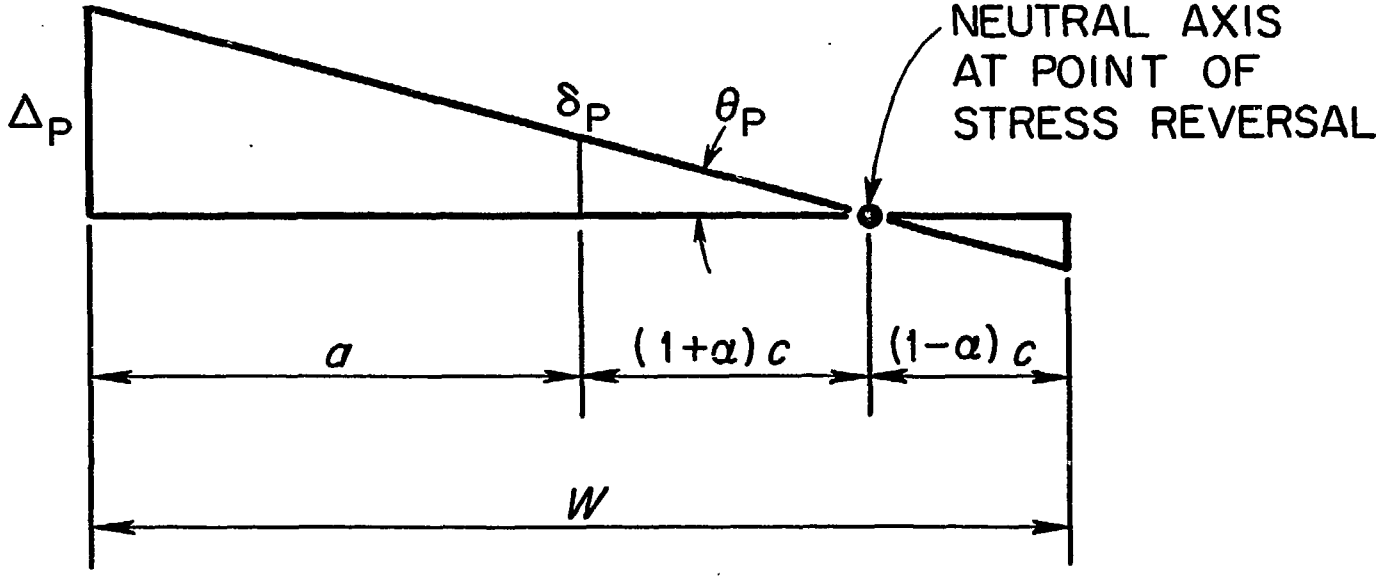

Figure 2

ORNL-DWG 74-110

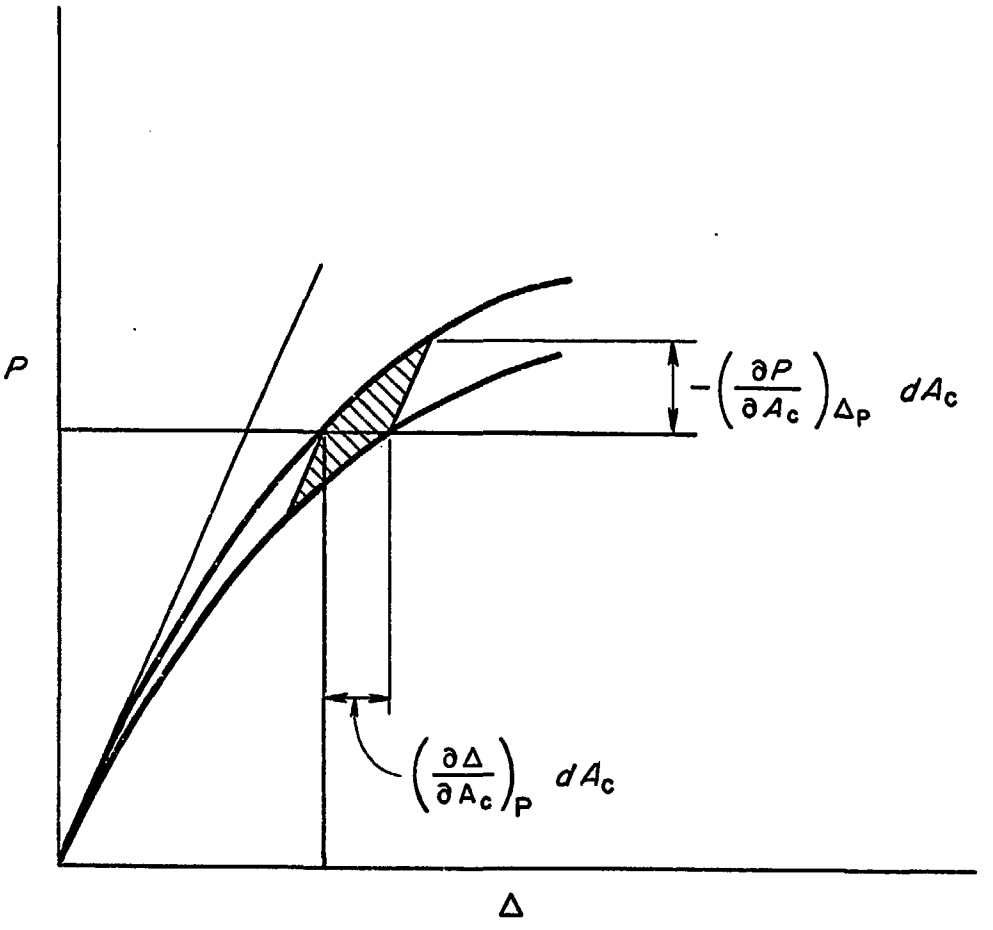

Figure 3

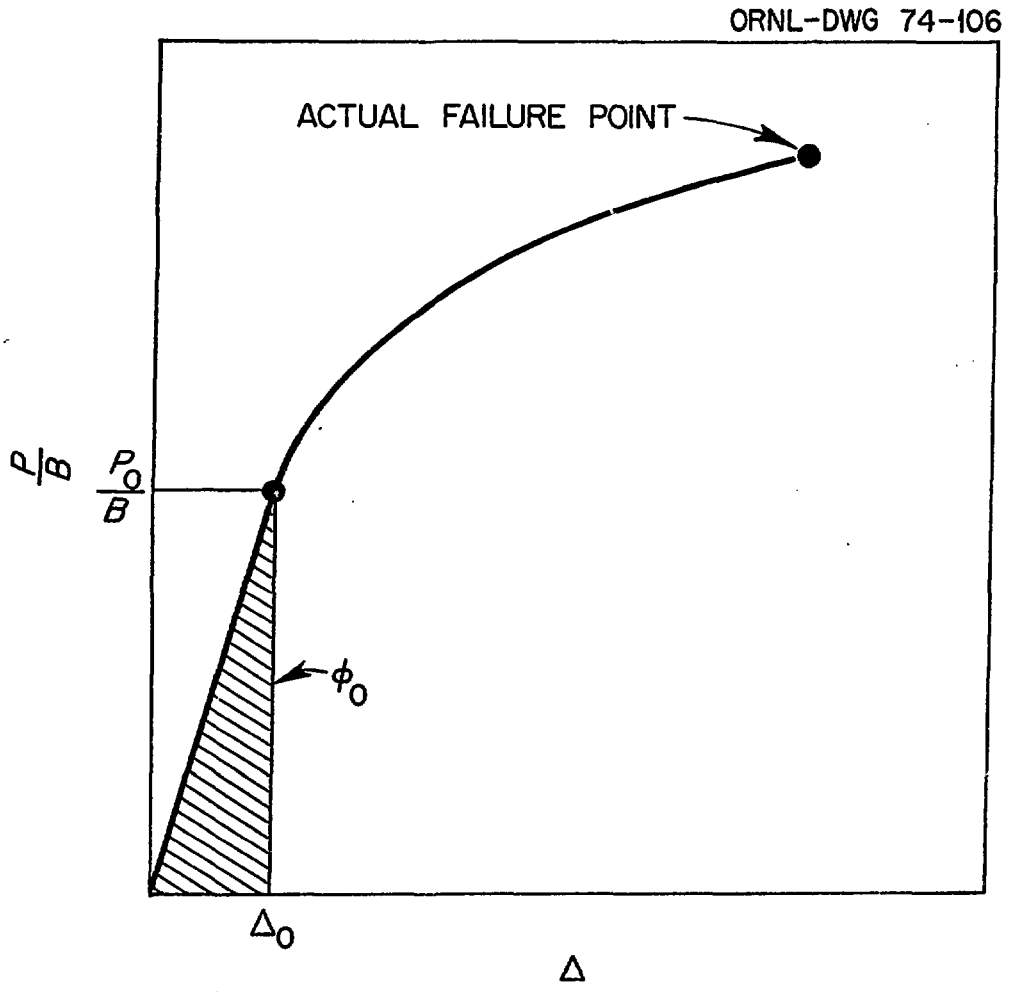

Figure 4

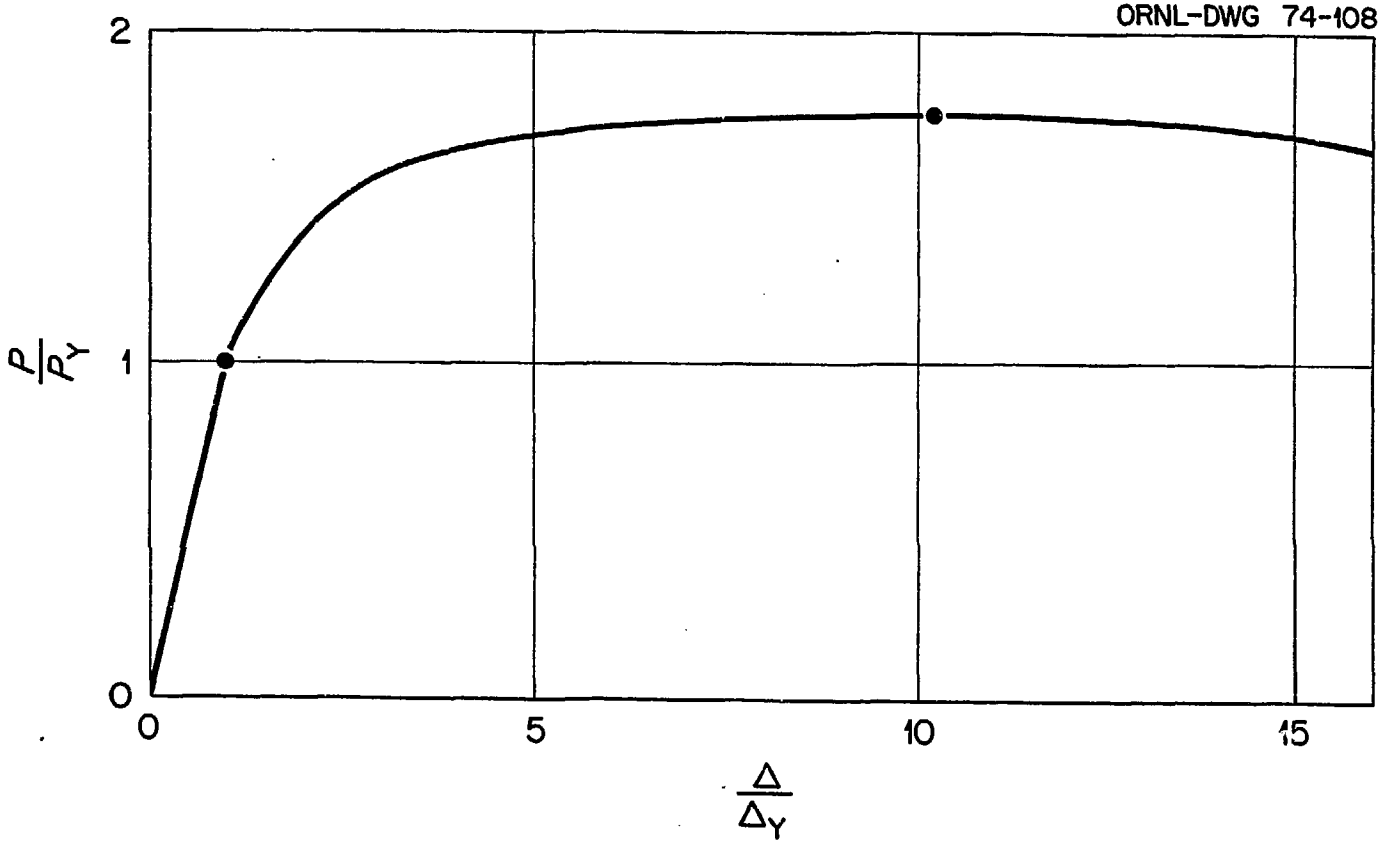

Figure

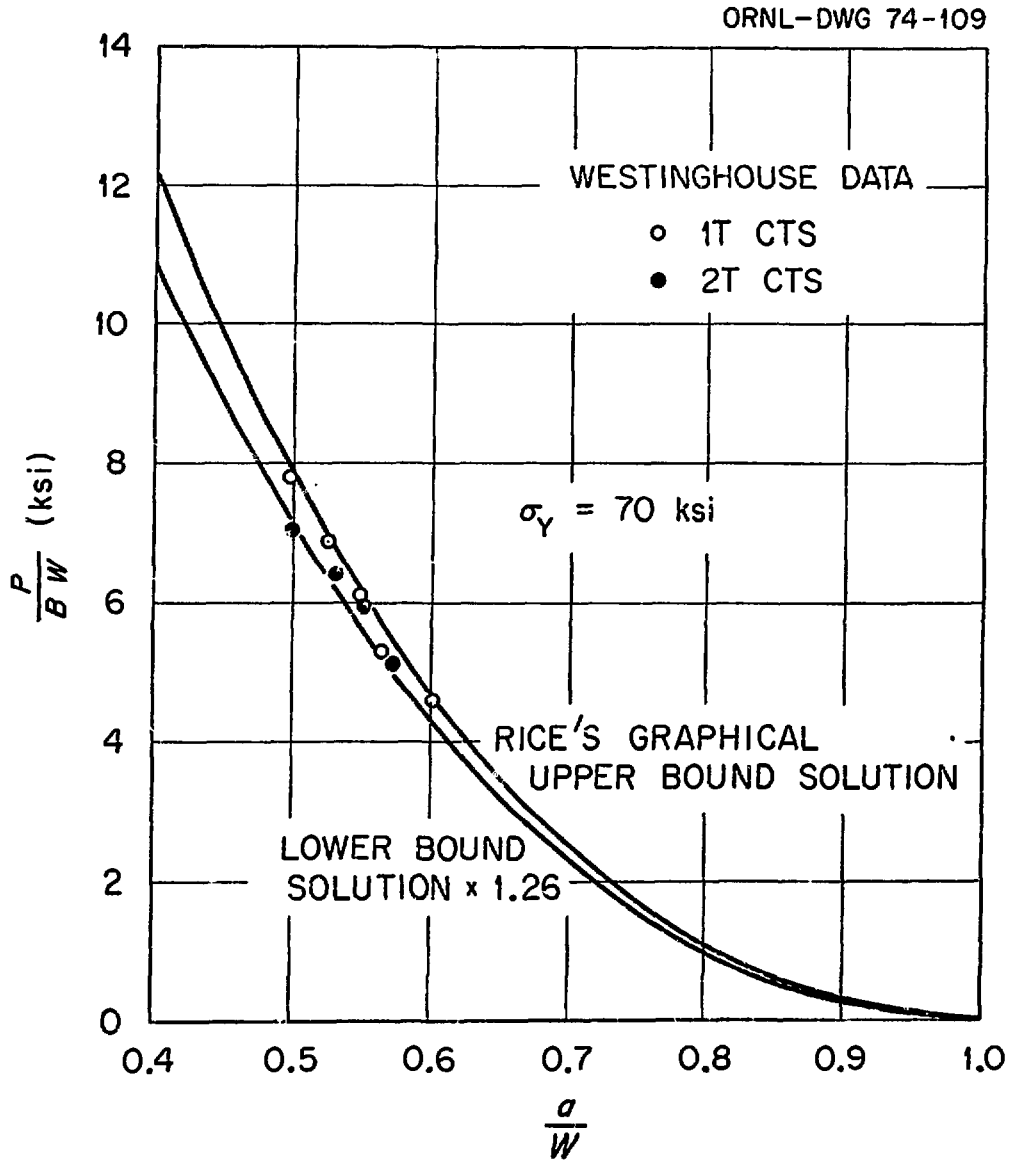
ORNL-DWG 74-109
WESTINGHOUSE DATA
1T CTS
2T CTS
σ_Y = 70 ksi
RICE'S GRAPHICAL
UPPER BOUND SOLUTION
LOWER BOUND
SOLUTION x 1.26
$\frac{P}{B\sqrt{W}}$ (ksi)
$\frac{a}{W}$
0
2
4
6
8
10
12
14
0.4
0.5
0.6
0.7
0.8
0.9
1.0

Figure A.1